ELSEVIER
manuscript PLA-D-18-01874

Physics Letters A

doi:10.1016/j.physleta.2018.11.008

Monodromy in non-integrable systems on certain compact classical phase spaces

Dmitriĭ A. Sadovskiĭ*, Boris I. Zhilinskiĭ

Département de physique, Université du Littoral – Côte d'Opale, 59140 Dunkerque, France

file: bpmono TEXed 2018-11-24 15:32, 6 pages
The final author version of the manuscript with 2 figures, 1 table, and 40 bibliography entries.

Abstract

On the example of bending vibrational polyads of the acetylene molecule (C_2H_2) in the approximation of the 1:1:1:1 resonant oscillator with axial symmetry, whose geometry is similar to the n-shell approximation of the perturbed hydrogen atom, we show how remaining invariant tori of the underlying classical non-integrable system form a nontrivial continuous family with monodromy. We read this monodromy off the quantum energy spectrum which was observed experimentally by spectroscopists, and we uncover its origins through the particular topology, geometry, and symmetry. We explain how monodromy characterizes the chaotic region surrounded by the tori. We detail the explicit correspondence between the bending polyads of C_2H_2 and the n-shells of the hydrogen atom, and uncover the dynamical SO(3) symmetry of the bending polyads and the corresponding spherically localized vibrational states.

Keywords: Hamiltonian monodromy, bending vibrational polyads of acetylene, complex hyperbolic equilibrium, integrable approximation, perturbations of the hydrogen atom, Kustaanheimo-Stiefel formalism

1. Introduction

A study of any classical Hamiltonian dynamical system and its quantum analog begins with investigating integrability. The presence of invariant tori, typical for integrable systems, is of primary interest of this examination. Locally, we are guaranteed to have action-angle variables on the tori, and the Einstein-Brillouin-Keller (EBK) action quantization gives us the corresponding quantum spectrum. Hamiltonian monodromy [1] characterizes how invariant tori fit together in the classical phase space. It allows to proceed from the simple local action-angle description towards the global geometric understanding of the classical dynamics. Similarly, quantum monodromy [2] incorporates local oscillator-like quantization into the representation of the entire spectrum of the corresponding quantum system. Specifically, systems with nontrivial monodromy, or simply—with monodromy, do not have globally single-valued and smooth action variables. The respective quantum system cannot be described using one global set of quantum numbers which are smooth in the limit $\hbar \to 0$. In the space of integrals, the quantum spectrum of this system is represented by a locally regular lattice with a defect [3].

The first study of a fundamental physical system with monodromy, the perturbed hydrogen atom [4, 5], relied on a conjecture, later confirmed [6, 7], that monodromy can describe the surviving Kolmogorov-Arnold-Moser (KAM) tori of perturbed integrable systems. This gave immediately an opening to analyze many important atomic and molecular systems, including rotating quasilinear molecules near their unstable linear equilibria, such as H_2O [8] and others [9], a rich class of systems with coupled slow-fast angular momenta [10], the H_2^+ ion [11], rotating dipolar symmetric top molecules and diatomic molecules subjected to an external electric field [12, 13], and resonant "swing-spring" vibrations of CO_2 [14]. Several pivotal generalizations followed [15–20], and similar concepts were introduced in other fields [21, 22]. Knowing dynamical connections across the families of invariant tori and the respective quantum states becomes decisive when the system is controlled through time-dependent perturbations [23].

2. Main statement

The most distinctively new general conjecture in our present work is *the possibility to introduce monodromy in specific globally non-integrable systems*. We formulate and develop our idea on the concrete physical example of bending vibrations of the acetylene molecule [24]. After reduction in the (1:1):(1:1) resonance approximation, this system has two degrees of freedom and compact four-dimensional classical phase space $\mathbb{S}^2\times\mathbb{S}^2$. We exploit the fact that in addition to stable (elliptic) equilibria, systems on $\mathbb{S}^2\times\mathbb{S}^2$, and, likewise, systems on $\mathbb{C}P^2$, another compact classical phase space with fundamental physical applications, possess continuous families of stable low-dimensional tori, or critical fibres $\mathbb{S}^1$. Adapting Nekhoroshev's terminology [17], we call these families "upper bounding walls", or simply—walls W. In our particular example [24], walls are fixed by additional discrete symmetries. Similarly to the saturated neighbourhoods of elliptic equilibria, domains of approximate integrability M exist near the walls, and, depending on the wall topology, or more specifically, depending on the singularities of the walls, regular KAM tori $\mathbb{T}^2$ within M may form a family with nontrivial monodromy, while the rest of the phase space is taken over by chaotic dynamics. In our concrete example,

*Corresponding author
Email addresses: sadovski@univ-littoral.fr (Dmitriĭ A. Sadovskiĭ), zhilin@univ-littoral.fr (Boris I. Zhilinskiĭ)

 submitted September 9, in final form Nov. 1, accepted Nov. 7, available online November 12, 2018

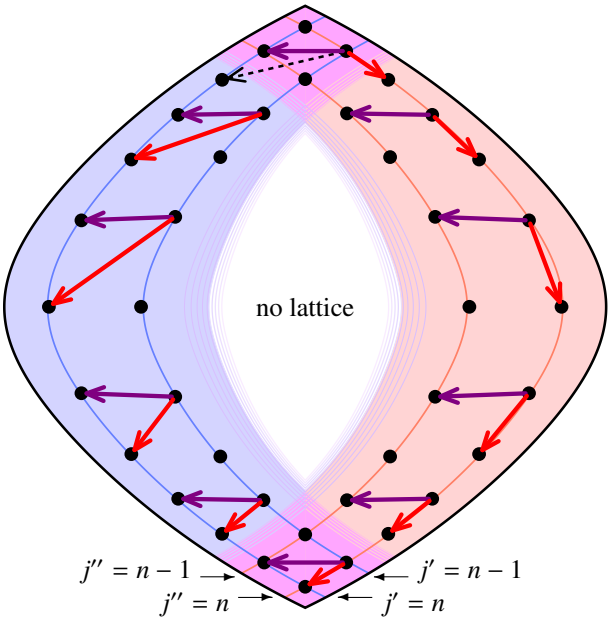

Figure 1: Quantum monodromy in a non-integrable system with walls (color online). The two shaded areas encased by bold solid lines represent the base of the combined toric fibration B and the lower bounding walls, respectively, in the image of the partial integral map $\mathcal{I}$. This particular arrangement corresponds to the example of the vibrational bending polyads of acetylene. Specifically, left and right quantum lattices model j' and j'' localized spherical states of polyad $N_b = 12$, and the integral defining the vertical axis corresponds to the vibrational energy (cf fig. 2). Arrows represent local lattice bases connected along the closed loop starting near the top vertex and going clockwise. Comparing the returning vectors (dashed lines) to the initial ones, we compute monodromy.

chaotic dynamics concentrates in the neighbourhoods of two complex-hyperbolic (focus-focus) equilibria. In general, it is the monodromy which we compute along the bounding walls that gives information on the inaccessible chaotic region.

In order to describe the foliation of M, let us introduce the mapping

$$\mathcal{I} : \overline{\mathsf{M}} \subseteq P \to B \subset \mathbb{R}^2 : (q,p) \mapsto (\mathcal{I}_1(q,p), \mathcal{I}_2(q,p))$$

which we can call a "partial integral map", and which differs from the more familiar momentum and/or energy-momentum maps in that (i) its range covers effectively only part of phase space P available to the system, and (ii) none of the integrals is necessarily a momentum (defining globally an $\mathbb{S}^1$ action on P). A constructive argument affirms the existence of map $\mathcal{I}$ in Hamiltonian dynamical systems on compact four-dimensional phase spaces P [24]: one of its integrals is readily available as energy, while the other can be constructed by extending local actions across the region of integrability M along the bounding wall $\mathsf{W} \subset \partial\mathsf{M}$.

The union of the integrability domains M and the walls can be considered as a fiber bundle whose base is the image of $\mathcal{I}$ and is a domain $B \subset \mathbb{R}^2$ bounded partially by the image of the walls, or "lower bounding walls", seen as curves in $\mathbb{R}^2$ (fig. 1). We consider closed loops going in the base near and along lower walls. Monodromy corresponding to these loops is a function of the singular points present on the wall[1]. We can expect results similar to the Duistermaat–Heckman theorem (as detailed in [25], see also [26, 27]). The quantum states which are localized near the wall form a locally regular $\mathbb{Z}^2$ lattice in the base domain B which may have monodromy (fig. 1).

To appraise the particular setup in fig. 1 and its concrete realization in sec. 3 below, let us turn to the elliptic equilibria on the compact phase spaces P which we consider here. These equilibria are bound to exist on P and Morse theory can supply more information on them. Near each such equilibrium, the system is approximated naturally as an oscillator. In two degrees of freedom, its bifurcation diagram is a familiar closed quarter plane

$$\overline{V} = \{(I_1, I_2) \in \mathbb{R}^2, I_1 \geq 0, I_2 \geq 0\}, \quad \partial V = \mathbb{R}_{\geq 0} \cup \mathbb{R}_{\geq 0},$$

whose interior points, vertex, and regular boundary points lift to regular tori, the equilibrium point O, and periodic orbits $\mathbb{S}^1$, respectively. The latter are critical lower-dimensional tori constituting two normal mode families. The preimage of the lower wall ∂V is the upper bounding wall which consists of two continuous $\mathbb{S}^1$ families contracting to the common point O. This can be seen as two two-dimensional surfaces in $\mathbb{R}^4$ intersecting generically in one point of the four-dimensional space. Under typical perturbations, the integrable oscillator approximation becomes increasingly inadequate away from O, but the two $\mathbb{S}^1$ families may continue and even remain critical. Let us now consider two elliptic equilibria O_+ and O_- at which the energy reaches its maximal and minimal values on P. They correspond to the upper and lower vertices in fig. 1 and to the normal modes of the concrete system in sec. 3. The fundamental premise of the structure in this figure is the assumption that the families of critical orbits coming out of O_+ and O_- *connect* so that we can continue from one equilibrium to another. As a result, the entire lower bounding wall is circular. Moreover, complemented with two critical points $O_\pm$, each connected $\mathbb{S}^1$ family constitutes a 2-sphere $\mathbb{S}^2 \subset P$. Consequently, the upper wall $\mathsf{W} \subset P$ is a non-simply connected joint union of two spheres, W' and W'', intersecting on $\{O_\pm\}$. Note that if an $\mathbb{S}^1$ orbit on W' or W'' goes hyperbolic as the dynamical parameter n increases, a part of the sphere will no longer be bounding (but rather form an internal wall) and we would have to follow a more complicated bounding wall. In the concrete system (sec. 3), several such phenomena occur at large n as Hamiltonian pitchfork bifurcations, and so in [24], we considered modified integrability domain M and base B to obtain similar results at larger n. Presently, we keep the most basic setup and do not discuss such situations.

Further assumptions behind fig. 1 are simplifying but not stringent and are inspired by the concrete example of bending polyads (sec. 3). Thus we can suppose that the spheres W' and W'' are smooth and can be equipped with a constant symplectic 2-form proportional to the area element. We choose actions j' and j'' which are conserved on the respective spheres, and which turn into oscillator actions I_1 and I_2 near the equilibria O. Because W' and W'' are critical, the respective actions j' and j'' reach their maximal constant values on them. For simplicity, we assume the latter to be equal, and we use the energy H to define a height function on each sphere. The above assumptions on the geometry of and the symplectic structure on W' and

W″ turn quantization into the standard procedure for the angular momentum. Quantum states localized near W′ (and/or W″) have values of quantum numbers $j' = n$ (and/or $j'' = n$) slightly below the classically allowed maximal value and form $2n + 1$ multiplets stretching along the respective parts of the lower wall in fig. 1. After excitation in the complementary degree of freedom, j' or j'' step down by 1 and we have $2n - 1$ multiplets. In the domains $V_\pm$ near maximum and minimum energies where j' and j'' become oscillator actions, the two resulting sublattices intersect in a precise way shown in fig. 1.

3. Bending vibrations of acetylene

We turn to our molecular example which demonstrates that the general scheme in fig. 1 has concrete physical realizations. Two doubly degenerate bending vibrations of acetylene C_2H_2 can be well approximated as a (1:1):(1:1) resonant oscillator with axial symmetry. Quantum states of this system form *polyads* characterized by polyad number N_b and angular momentum ℓ. They were investigated extensively by spectroscopists [28]. The underlying dynamics was also scrutinized in depth [29–31], see our recent paper [24] for a review and complete references. However, the geometry of the underlying reduced classical system with two degrees of freedom was not fully described. We show in [24] that this system is equivalent to the Keplerian n-shell approximations (for a detailed introduction, see [32] and citations therein). The equivalence is explicit in the Kustaanheimo-Stiefel (KS) variables. So, in particular, n-shells of the hydrogen atom correspond to polyads with $\ell = 0$ and $N_b = 2(n - 1)$. Unless we allow for magnetic monopoles, polyads with $\ell > 0$ have no such analogs but have the same reduced phase space topology $\mathbb{S}^2\times\mathbb{S}^2$ [24].

On the other hand, we note an important dynamical difference between Stark-Zeeman perturbations of the hydrogen atom and bending polyads: while the former have an additional smallness parameter rooted in the specific scaling of perturbations with n [32], no such scaling occurs for vibrations. So, generally, no approximate "third" integral of motion can be expected to exist in addition to (N_b, ℓ), and there are strong reasons to believe—and many researchers did so—that the internal polyad dynamics for large $N_b \geq 10$ is entirely irregular. This is why our discovery of dynamical symmetries and monodromy in this system is an important result.

Our analysis in [24] relied on the methods developed earlier [32] and required substantial technical developments. In the present paper, we refine the argument of [24] and reveal its geometric elegance and generality which deserve attention across different fields of dynamical theory, atomic and molecular physics, mechanics, and mathematics.

The bending polyad system on $\mathbb{S}^2\times\mathbb{S}^2$ inherits discrete symmetries of the molecule. Their analysis gives important clues to the dynamics [24]. Invariant subspaces of $\mathbb{S}^2\times\mathbb{S}^2$ with purely spatial, and therefore symplectic, nontrivial isotropy are of primary interest. These include four isolated fixed points, or *poles* and two spheres $\mathsf{W}' := \mathbb{S}^2_{j'}$ and $\mathsf{W}'' := \mathbb{S}^2_{j''}$ with stabilizers of order 2. Using vectors $\boldsymbol{L} = (L_1, L_2, L_3)$ and $\boldsymbol{K} = (K_1, K_2, K_3)$

Table 1: Part of the vibrational bending polyad Hamiltonian of C_2H_2 which includes terms up to degree 2 in dynamical variables $\{\boldsymbol{K}, \boldsymbol{L}\}$ and is restricted to $\ell = 0$. Parameters are adjusted to reproduce the data [28] for $2(n-1) = N_b \leq 14$ to their accuracy of 0.05 cm^{-1}.

Term	Parameter cm^{-1}	Term	Parameter cm^{-1}
n	1332.0650(62)	K_1	120.310(11)
$(j')^2$	5.7669(15)	n^2	−4.1318(23)
ξ'	−6.167(13)	nK_1	−11.7249(59)
ξ''	−2.1702(69)		
L_1^2	0.0604(23)	K_1^2	0.4259(20)

which obey the relations

$$\boldsymbol{K} \cdot \boldsymbol{L} = 0 \quad \text{and} \quad \boldsymbol{K}^2 + \boldsymbol{L}^2 = n^2,$$

and which represent the angular momentum and the eccentricity, respectively, in Keplerian systems [32], as coordinates and dynamical variables, we find that $(\boldsymbol{K}, \boldsymbol{L})$ equal $(\pm(n, 0, 0), \boldsymbol{0})$ and $(\boldsymbol{0}, \pm(n, 0, 0))$ at the poles. While the $K_1 = \pm n$ poles correspond to two different critical one-point orbits of the symmetry group action, a spatio-temporal symmetry makes the $L_1 = \pm n$ poles equivalent and they form one two-point orbit. The spheres are maximal constant n-level sets of the norms j' and j'' of respective vectors

$$\boldsymbol{J}' = (K_1, L_2, K_3) \quad \text{and} \quad \boldsymbol{J}'' = (K_1, K_2, L_3).$$

They intersect each other in $\{K_1 = \pm n\}$ and form a joint union space W with one nontrivial 1-cycle. We will see that W is the upper bounding wall whose image is a circle with two singular points corresponding to $\{K_1 = \pm n\}$, and that this image constitutes the lower wall (solid boundary in fig. 1).

The poles are necessarily equilibria for any bending vibrational polyad [24]; their dynamical characterization was well understood [29–31]: $\{K_1 = \pm n\}$ correspond to two bending normal modes and $\{L_1 = \pm n\}$ represent a circular nonlinear mode. At low excitations, the system is governed by the large linear detuning term K_1 (see table 1) whose parameter reflects the frequency difference of the two bending normal modes. The system has four equilibria, the minimum number on $\mathbb{S}^2\times\mathbb{S}^2$ [24]; $\{K_1 = \pm n\}$ are elliptic with maximal (for $K_1 = n$) and minimal (for $K_1 = -n$) energy within the polyad, while $\{L_1 = \pm n\}$ are complex hyperbolic. Higher up, in the interval of $n = 7 \ldots 10$, the quadratic part of the reduced Hamiltonian begins to dominate and several bifurcations occur at the poles. In particular, "local modes" emerge at $\{K_1 = \pm n\}$ [24, 29–31] thus destroying any chances for K_1 to serve as an approximate global third integral (momentum).

The importance of the two spheres $\mathbb{S}^2_{j'}$ and $\mathbb{S}^2_{j''}$ with a symplectic isotropy group was uncovered in [24]. These spaces are *dynamically invariant*, i.e., the trajectories of the system do not leave them and foliate them into constant energy level sets which are, generically, circles $\mathbb{S}^1$ (periodic orbits). In an integrable system, this constitutes two continuous families of critical (lower-dimensional) fibres. Recalling how $\mathsf{W} = \mathbb{S}^2_{j'} \cup \mathbb{S}^2_{j''}$ is connected, we obtain one united family.

The Poisson structure matches constructively our interesting geometry. We observe that vectors $\boldsymbol{J}'$ and $\boldsymbol{J}''$ represent two

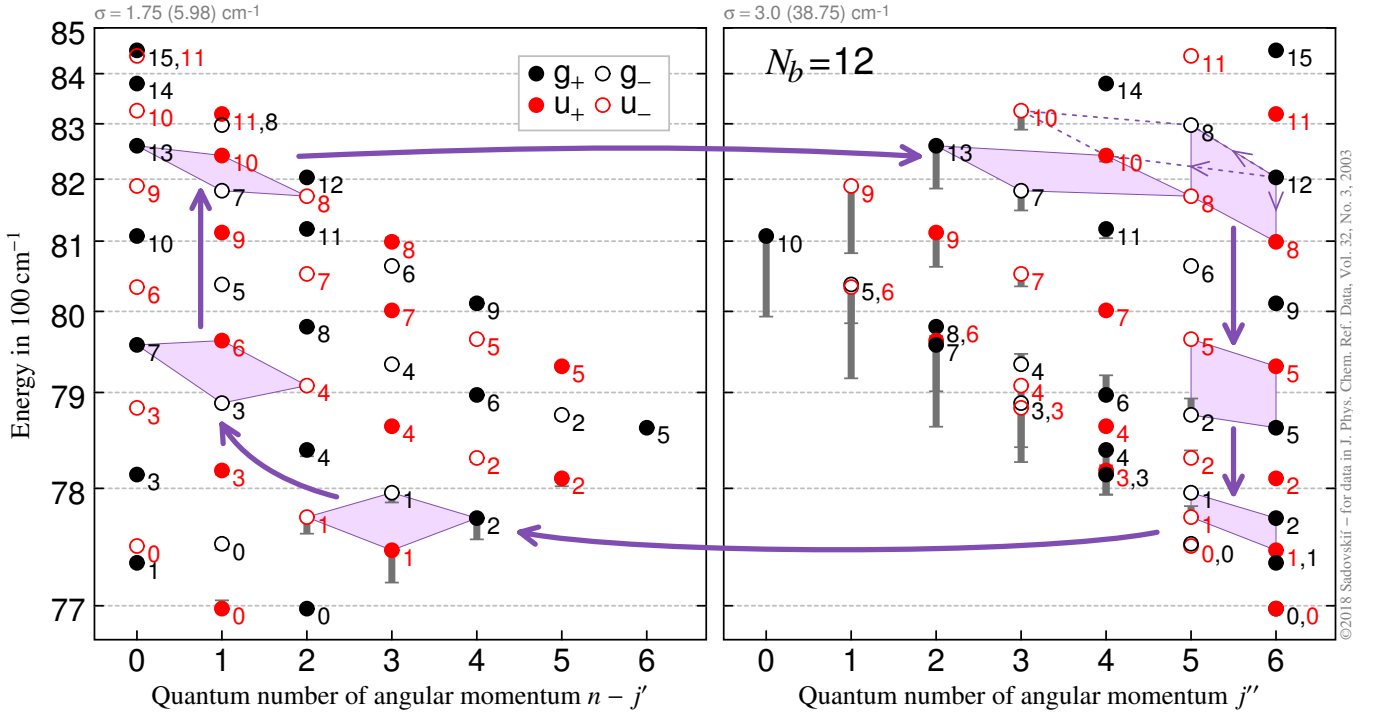

Figure 2: Quantum lattices of bending vibrational states of polyad $N_b = 12$, $\ell = 0$ of acetylene in the approximation with third integral j' (left) and j'' (right). Lattice nodes (circles, color online) represent energy levels [28] of four different symmetry species; gray vertical bars display errors of the integrable approximation to each state. The nodes in the j' and j'' panels can be identified using the subscripts which give unique multiplicity indices of the eigenstates within their symmetry type. Elementary lattice cells (shaded quadrangles) and arrows illustrate the computation of monodromy according to the scheme in fig. 1. The energy axis nonlinearity facilitates understanding the lattice structure. The initial and final cell bases (mid-side arrow heads) correspond to those in fig. 1.

angular momenta. Indeed, their components span two distinct so(3) subalgebras of so(4) with Casimirs j' and j''. The latter satisfy the relation

$$(j')^2 + (j'')^2 + L_1^2 - K_1^2 = n^2$$

and do not Poisson commute. Near W, they can be assimilated with local actions, one of which remains large and constant along W′ or W″. Because this large action attains its maximal value $N_b/2$ on the respective sphere, W is a bounding wall. On each sphere W′ and W″, we have a one-degree-of-freedom restricted dynamical system whose equations of motion are Euler-Poisson equations for the components of $\boldsymbol{J}'$ and $\boldsymbol{J}''$, respectively. This is similar to the reduced freely rotating rigid body (the Euler top) and to the polyads of doubly degenerate oscillators, albeit here we have specific restricted contributions from *two* doubly degenerate normal modes in near 1:1 resonance.

The Hamiltonian for a N_b-polyad with $\ell = 0$ can be written in terms of j' or j'', and ξ', ξ'', K_1, and L_1^2 (table 1), where

$$\xi' = L_2^2 - K_3^2 \quad \text{and} \quad \xi'' = L_3^2 - K_2^2$$

Poisson commute with j' and j'', respectively. The non-commuting terms vanish on W. So, in particular, the restricted Hamiltonian $\mathcal{H}'_n : \mathsf{W}' \to \mathbb{R}$ is a function of j', ξ', K_1. This Hamiltonian describes exactly the dynamics on W′, but it can also be used to approximate the dynamics in the neighbourhood of W′ where j' is large (cf. left shaded domain in fig. 1). Similarly, $\mathcal{H}''_n : \mathsf{W}'' \to \mathbb{R}$ is a function of j'', ξ'', K_1 describing the dynamics on and near W″ where j'' is large (right shaded domain in fig. 1). Both approximations apply simultaneously near the poles $\{K_1 = \pm n\}$ where both j' and j'' are large (vertices in fig. 1). On the other hand, since both j' and j'' vanish in $\{L_1 = \pm n\}$, both approximations fail in the sufficiently small open neighbourhoods $\Sigma_\pm$ of $\{L_1 = \pm n\}$. This strongly suggests that the dynamics in $\Sigma_\pm$ is chaotic.

The quality of the above integrable approximations and the extent of the integrability domain $\mathsf{M} = \mathsf{M}' \cap \mathsf{M}''$ near W depend on the parameters of the non-commuting terms. Thus we can see from table 1 that when we use j', the parameter of L_1^2 becomes *anomalously* small while that of ξ'' is quite moderate. This means that the bending vibrational polyad system of acetylene has *dynamical symmetry* SO(4) ⊃ SO(3) with additional good quantum number (momentum) j' [24]. On the other hand, the j'' approximation is less global. This approximation averages out large ξ' and L_1^2 contributions, and has a substantial quadratic term K_1^2.

In order to see how the two integrable approximations reproduce the polyad states, we treated $\mathcal{H}'$ and $\mathcal{H}''$ as effective Hamiltonians and re-adjusted their parameters attributing higher weights to levels with large j' and j'', respectively. Our results for $N_b = 12$ are presented in fig. 2 as two complementary energy-momentum lattices[2] whose $(2j+1)$–point columns correspond to multiplets of states with the same momentum $j = j'$ or j''. The largest-j multiplet (leftmost or rightmost column in fig. 2) is constituted by the levels localized near the walls W′ or W″, and represents most closely the restricted dynamics on

the respective spheres. Near the maximal and minimal energies, we observe doublets which correspond to local modes created after bifurcations at the poles $\{K_1 = \pm n\}$. We can see that the j' approximation in fig. 2, left reproduces almost all energies, its errors of 1–5 cm^{-1} being negligible in the scale of the plot. The j'' approximation is visibly in trouble at low j'', but for the maximal $j'' = N_b/2$ and the one below it, the errors remain low, within 3 cm^{-1}. This confirms the dynamical stability of bounding walls W.

4. Computation of monodromy

We continue exploring the $N_b = 12$ energy-momentum lattices in fig. 2. Like two charts, they represent differently the same multiplet of $(N_b/2+1)^2 = 49$ quantum eigenstates whose symmetry type and additional multiplicity index (within the group of states of the same symmetry sorted by energy) identify them unambiguously. For the maximum momentum $j = N_b/2$ with $j = j'$ or j'', the lattices can be used adequately to follow the states localized near W. Since the components of W are $\mathbb{S}^2$ spheres, we can call such states *spherically localized*. Near the maximal and the minimal energies of the shell, or simply near the poles $\{K_1 = \pm n\}$, the j' and j'' lattices overlap, and either lattice can be used so that we can switch between them. In fact, momenta (j', j'') give the choice of local actions of the doubly degenerate oscillators at $\{K_1 = \pm n\}$. The states with large $(j', j'') \approx N_b/2$ have, therefore, stronger localization. Specifically, they are localized near the elliptic equilibria $\{K_1 = \pm n\}$ when N_b is low, or near and within the local structures emerging after these equilibria undergo supercritical Hamiltonian pitchfork bifurcations. We observe that maximal-j states correspond to the outermost points of the lattices. So the $j'' = N_b/2$ states follow the two-piece smooth right boundary of the j' lattice in fig. 2, left. At the same time, the $\langle L_1 \rangle$ values suggest that the complex hyperbolic poles $\{L_1 = \pm n\}$ together with their neighbourhoods $\Sigma_\pm$ map into the interior of the low-j domains. It also follows that at low N_b, near the maximal and minimal energy, the lattices overlap precisely as in the model in fig. 1, i.e., like a $\mathbb{Z}^2$ lattice filling a quarter-plane. This allows connecting local quantum numbers within the family of spherically localized $N_b, \ell = 0$ shell eigenstates, see figs. 1 and 2, and computing monodromy. In the appropriately chosen initial local action basis (figs. 1 and 2), for a closed path that follows the image of the wall W, the resulting monodromy matrix is

$$\begin{pmatrix} 1 & 2 \\ 0 & 1 \end{pmatrix}.$$

This computation is illustrated by the elementary cell transport in fig. 2. Comparing to its predecessor, fig.10 of [24], we use a slightly different path in fig. 2 in order to avoid the region of local mode doublets in the j'' lattice which appear at $N_b > 10$, and to follow a more straightforward approach represented schematically in fig. 1.

5. Conclusions

With regard to the similar earlier results in systems with (approximate) global integrability [5], the near-integrable KAM systems [6, 7], and the most recent variation on the theme [33], we like to point out that in contrast to figures 3 and 9 in [5] and other similar figures of global lattices with defects, our fig. 1 presents *two* overlapping $\mathbb{Z}^2$ lattices which do not share the momentum integral and do not cover the whole spectrum. Furthermore, in the past, the off-diagonal element of the monodromy matrix was associated with the presence of the particular singular fiber(s) whose image gets encircled in the base of the fibration [5, 10, 32, 33]. The idea came from the geometric monodromy theorem [34] and similar statements in the general singularity theory [35] which treated monodromy as global consequence of local singularities or singular fibres. In the Hamiltonian framework, the latter correspond, most generically, to the *pinched torus*, the homoclinic connection of the stable and unstable manifolds of the focus-focus equilibrium. Its counterpart in the Picard-Lefschetz singularity theory is the A_1 singularity. In our present work, while neither singular nor regular invariant tori persist in the neighbourhoods $\Sigma_\pm$ of the focus-focus equilibria $\{L_1 = \pm n\}$, we examine monodromy directly, globally, away from $\Sigma_\pm$. In this respect, our approach is similar to that of [25] where monodromy is consistently related to the polytope boundaries of the base of the fibration. Considering general (singular) Lagrangian fibrations with compact total spaces [36, 37], we like to repeat that our analysis concerns primarily systems on compact symplectic 4-manifolds $\mathbb{S}^2\times\mathbb{S}^2$ and $\mathbb{C}P^2$ which allow bounding walls and have many important known physical realizations. The $\mathbb{S}^2\times\mathbb{S}^2$ examples include perturbed Keplerian systems, such as the hydrogen atom discussed here, or Rydberg atoms and molecules, resonant bending vibrational modes of molecules, notably those of linear molecules C_2H_2 or C_2N_2, vibration-rotation systems [38], specifically the rotational structure of vibrational polyads formed by doubly degenerate modes, and last but not least, various coupled angular momentum systems [10]. The $\mathbb{C}P^2$ examples concern the structure of vibrational polyads formed by triply degenerate vibrational modes of molecules (notably highly symmetric molecules SF_6, CH_4 [39], and others) or nuclei, or quasi-degenerate modes of simpler molecular systems, for example O_3 [40].

Acknowledgments

We thank the referees for their pertinent comments which helped to improve the manuscript.

Notes

1 With each singular boundary point, we can associate (isolate) a monodromy matrix contribution which may depend on the type of the singularity, and specifically, on its isotropy (stabilizer). Once contributions from all singular points on the boundary are established, the monodromy map associated with a cyclic path along the boundary can be defined without any additional contributions coming from the regular parts of the boundary.

2 Comparing fig. 2 to fig.10 of [24], we note the difference in the momenta. The latter are introduced in [24] as extrapolated local actions and are related to j' and j''. We should also notice the two interchanged points $g_{+,0}$

and $g_{+,1}$ in the lower part of the j' lattice. Their present placement is in better agreement with the expectation values of $\langle K_1 \rangle$ and $\langle (j')^2 \rangle$ in the exact spectrum.

References

[1] J. J. Duistermaat, On global action-angle coordinates, Comm. Pure Appl. Math. 33 (6) (1980) 687–706.

[2] R. H. Cushman, J. J. Duistermaat, The quantum-mechanical spherical pendulum, Bull. Am. Math. Soc. 19 (1988) 475–479.

[3] B. I. Zhilinskiĭ, Hamiltonian monodromy as lattice defect, in: M. I. Monastyrsky (Ed.), Topology in Condensed Matter, Vol. 150 of Springer Series in Solid-State Sciences, Springer, Berlin, Heidelberg, 2006, pp. 165–186. doi:10.1007/3-540-31264-1_8.

[4] R. H. Cushman, D. A. Sadovskiĭ, Monodromy in perturbed Kepler systems: hydrogen atom in crossed fields, Europhys. Lett. 47 (1999) 1–7.

[5] R. H. Cushman, D. A. Sadovskiĭ, Monodromy in the hydrogen atom in crossed fields, Physica D 142 (2000) 166–96.

[6] B. W. Rink, A Cantor set of tori with monodromy near a focus–focus singularity, Nonlinearity 17 (1) (2004) 347–356.

[7] H. Broer, R. Cushman, F. Fassò, F. Takens, Geometry of KAM tori for nearly integrable Hamiltonian systems, Erg. Theor. Dyn. Syst. 27 (2007) 725–741.

[8] M. S. Child, T. Weston, J. Tennyson, Quantum monodromy in the spectrum of H_2O and other systems: new insight into the level structure of quasi-linear molecules, Mol. Phys. 96 (1999) 371–379.

[9] B. P. Winnewisser, M. Winnewisser, I. R. Medvedev, M. Behnke, F. C. De Lucia, S. C. Ross, J. Koput, Experimental confirmation of quantum monodromy: The millimeter wave spectrum of cyanogen isothiocyanate NCNCS, Phys. Rev. Lett. 95 (2005) 243002.

[10] D. A. Sadovskiĭ, B. I. Zhilinskiĭ, Monodromy, diabolic points, and angular momentum coupling, Phys. Lett. A 256 (1999) 235–44.

[11] H. Waalkens, H. R. Dullin, P. H. Richter, The problem of two fixed centers: bifurcations, actions, monodromy, Physica D 196 (2004) 265–310.

[12] I. N. Kozin, R. M. Roberts, Monodromy in the spectrum of a rigid symmetric top molecule in an electric field, J. Chem. Phys. 118 (23) (2003) 10523–10533.

[13] C. A. Arango, W. W. Kennerly, G. S. Ezra, Quantum monodromy for diatomic molecules in combined electrostatic and pulsed nonresonant laser fields, Chem. Phys. Lett. 392 (4) (2004) 486–492.

[14] R. H. Cushman, H. R. Dullin, A. Giacobbe, D. D. Holm, M. Joyeux, P. Lynch, D. A. Sadovskiĭ, B. I. Zhilinskiĭ, CO_2 molecule as a quantum realization of the 1:1:2 resonant swing-spring with monodromy, Phys. Rev. Lett. 93 (2004) 024302/1–4.

[15] M. Joyeux, D. A. Sadovskiĭ, J. Tennyson, Monodromy of the LiNC/NCLi molecule, Chem. Phys. Lett. 382 (2003) 439–42.

[16] N. N. Nekhoroshev, D. A. Sadovskiĭ, B. I. Zhilinskiĭ, Fractional monodromy of resonant classical and quantum oscillators, C. R. Acad. Sci. Paris, Sér. I 335 (11) (2002) 985–8.

[17] N. N. Nekhoroshev, D. A. Sadovskiĭ, B. I. Zhilinskiĭ, Fractional Hamiltonian monodromy, Ann. H. Poincaré 7 (2006) 1099–211.

[18] D. A. Sadovskiĭ, B. I. Zhilinskiĭ, Hamiltonian systems with detuned 1:1:2 resonance: Manifestation of bidromy, Ann. Phys. 322 (2007) 164–200.

[19] K. Efstathiou, D. A. Sadovskiĭ, B. I. Zhilinskiĭ, Classification of perturbations of the hydrogen atom by small static electric and magnetic fields, Proc. Roy. Soc. London, Ser. A 463 (2007) 1771–1790.

[20] K. Efstathiou, O. V. Lukina, D. A. Sadovskiĭ, Most typical 1:2 resonant perturbation of the hydrogen atom by weak electric and magnetic fields, Phys. Rev. Lett. 101 (2008) 253003/1–4.

[21] H. R. Dullin, H. Waalkens, Nonuniqueness of the phase shift in central scattering due to monodromy, Phys. Rev. Lett. 101 (2008) 070405/1–4.

[22] D. Sugny, A. Picozzi, S. Lagrange, H. R. Jauslin, Role of singular tori in the dynamics of spatiotemporal nonlinear wave systems, Phys. Rev. Lett. 103 (2009) 034102.

[23] M. P. Nerem, D. Salmon, S. Aubin, J. B. Delos, Experimental observation of classical dynamical monodromy, Phys. Rev. Lett. 120 (2018) 134301.

[24] D. A. Sadovskiĭ, B. I. Zhilinskiĭ, Qualitative models of intramolecular dynamics of acetylene: relation between the bending polyads of acetylene and perturbed Keplerian systems, Mol. Phys. 116 (23-24) (2018) 3564–3601.

[25] S. Vũ Ngọc, Moment polytopes for symplectic manifolds with monodromy, Adv. Math. 208 (2007) 909–934.

[26] L. Grondin, D. A. Sadovskiĭ, B. I. Zhilinskiĭ, Monodromy as topological obstruction to global action-angle variables in systems with coupled angular momenta and rearrangement of bands in quantum spectra, Phys. Rev. A 65 (2002) 012105/1–15.

[27] A. Giacobbe, R. H. Cushman, D. A. Sadovskiĭ, B. I. Zhilinskiĭ, Monodromy of the quantum 1:1:2 resonant swing spring, J. Math. Phys. 45 (2004) 5076–100.

[28] M. Herman, A. Campargue, M. I. E. Idrissi, J. V. Auwera, Vibrational spectroscopic database on acetylene, $\tilde{X}\,{}^1\Sigma_g^+$ ($^{12}C_2H_2$, $^{12}C_2D_2$, and $^{13}C_2H_2$), J. Phys. Chem. Ref. Data 32 (3) (2003) 921–1361.

[29] V. Tyng, M. E. Kellman, Bending dynamics of acetylene: new modes born in bifurcations of normal modes, J. Phys. Chem. B 110 (38) (2006) 18859–71.

[30] V. Tyng, M. E. Kellman, Bifurcation phase diagram for C_2H_2 bending dynamics has a tetracritical point with spectral patterns, J. Phys. Chem. A 114 (36) (2010) 9825–9831.

[31] M. P. Jacobson, C. Jung, H. S. Taylor, R. W. Field, State-by-state assignment of the bending spectrum of acetylene at 15.000 cm^{-1}: A case study of quantum-classical correspondence, J. Chem. Phys. 111 (1999) 600–618.

[32] K. Efstathiou, D. A. Sadovskiĭ, Normalization and global analysis of perturbations of the hydrogen atom, Rev. Mod. Phys. 82 (3) (2010) 2099–2154.

[33] H. R. Dullin, H. Waalkens, Defect in the joint spectrum of hydrogen due to monodromy, Phys. Rev. Lett. 120 (2018) 020507.

[34] R. H. Cushman, J. J. Duistermaat, Non-Hamiltonian monodromy, J. Diff. Eqs. 172 (1) (2001) 42–58.

[35] D. A. Sadovskiĭ, Nekhoroshev's approach to Hamiltonian monodromy, Reg. & Chao. Dyn. 21 (6) (2016) 720–759.

[36] M. Symington, Four dimensions from two in symplectic topology, in: G. Matic, C. McCrory (Eds.), Topology and geometry of manifolds, Vol. 71 of Proc. Sympos. Pure Math., Amer. Math. Soc., Providence, Rhode Island, 2003, pp. 153–208. doi:10.1090/pspum/071.

[37] N. C. Leung, M. Symington, Almost toric symplectic four-manifolds, J. Symplectic Geom. 8 (2) (2010) 143–187.

[38] H. Crogman, V. Boudon, D. A. Sadovskiĭ, Local modes of silane within the framework of stretching vibrational polyads, Europ. Phys. J. D 42 (2007) 61–72.

[39] D. A. Sadovskiĭ, D. N. Kozlov, P. P. Radi, Direct absorption transitions to highly excited polyads 8, 10, and 12 of methane, Phys. Rev. A 82 (2010) 012503/1–17.

[40] I. N. Kozin, D. A. Sadovskiĭ, B. I. Zhilinskiĭ, Assigning vibrational polyads using relative equilibria: application to ozone, Spectrochim. Act. A 61 (2005) 2867–85.